Core-to-Rydberg excitations and their Auger decay in the HCl and DCl molecules

E. Kukk, H. Aksela, O.-P. Sairanen, E. Nõmmiste,* and S. Aksela
Department of Physical Sciences, Oulu University, FIN-90570 Oulu, Finland

S. J. Osborne, A. Ausmees,* and S. Svensson
Department of Physics, Uppsala University, Box 530, S-75121 Uppsala, Sweden
(Received 29 March 1996)

The resonant Auger electron spectra of the HCl and DCl molecules have been measured at the first core-to-Rydberg resonances. The low binding energy region of the spectra has been decomposed into transitions to different bound states and their vibrational progressions. Several transitions have been assigned using the strict spectator model. The total ion yield spectrum of HCl in the energy region of the core-to-Rydberg resonances has been recorded and its assignment refined with the help of the Auger electron and chlorine $2p$ photoelectron spectra. [S1050-2947(96)05209-2]

PACS number(s): 32.80.Hd

I. INTRODUCTION

The chlorine $2p$ photoabsorption, [1,2] total ion yield [3], and electron energy-loss spectra [4] of the HCl molecule show a number of narrow peaks, assigned to the core excitations to the s, p, and d Rydberg orbitals. The use of tunable synchrotron radiation allows one to selectively create various core-excited states, which decay mainly via molecular resonant Auger processes, populating the HCl^+ states with vacancies in the 4σ, 5σ, and 2π valence orbitals and an electron in a Rydberg orbital.

An earlier measurement [5] of the molecular Auger electron spectra from the decay of the core-excited states suffered from moderate electron and photon energy resolution (0.5-eV spectrometer broadening and 0.5-eV photon bandwidth), so that only a rather general description could be given. Recent progress in the instrumentation of electron spectroscopy and synchrotron radiation experiments has allowed these spectra to be recorded with much better resolution and quality, in particular by removing several simultaneous excitations of nearby Rydberg states. It is also useful to compare the spectra of HCl and DCl, as their different vibrational characteristics reveal which peaks in the spectra arise from different electronic transitions and which ones are merely the vibrational progressions accompanying them. The recent high-resolution measurements of Ar $2p^{-1}4s,3d$ Auger decay spectra [6] together with advanced atomic multiconfiguration Dirac-Fock (MCDF) calculations [7] provide a useful reference when interpreting the features in the molecular resonant Auger spectra.

Although the principal features of the chlorine $2p$ photoabsorption spectrum of HCl are known, several details still need clarification. For example, quite different strengths were assigned to the $2p_{1/2}\rightarrow 4s$ and $2p_{3/2}\rightarrow 3d$ transitions in photoabsorption [2] and electron energy-loss spectra [4]. The reason for such a discrepancy is that these transitions occur at almost the same photon energy, the corresponding absorption peaks are strongly overlapping and their intensity ratio is difficult to determine reliably. High-resolution electron spectroscopy is a valuable aid here, since the nature of the core excitations can be traced back from the resonant Auger decay patterns.

The molecular field splitting of the core orbitals, although weak, has been found to play an essential role in the $3d$ excitations to Rydberg orbitals and in their Auger decay in the HBr molecule [8]. The molecular field splitting of the Cl $2p$ orbital has been observed recently in the photoelectron and normal Auger spectra of HCl and DCl molecules, [9] but it has not been, as far as we know, utilized in the interpretation of the $2p$ photoabsorption features. The present resonant Auger spectra together with the $2p$ photoelectron spectrum [9] are used in this work to refine the assignment of the core excitations below the chlorine $2p$ ionization threshold in our total ion yield spectrum.

II. EXPERIMENTAL SETUP

The spectra have been measured at the Finnish beamline (BL 51) at MAX-I storage ring in Lund, Sweden [10,11]. Synchrotron radiation in the photon energy range 60–600 eV, obtained from a short-period undulator, is monochromatized by a modified SX-700 plane grating monochromator [12]. The beamline is equipped with a differential pumping section that reduces the pressure by five orders of magnitude between the experimental station and the monochromator. The spectra were recorded with a hemispherical sector electron analyzer [13], mounted at the magic angle relative to the electric vector of the photon beam. Electrons were retarded to a constant pass energy of 20 eV by using a lens system before the analyzer, which gave an electron energy resolution of about 65 meV. The electron spectra were recorded at the 50-μm exit slit width of the monochromator, corresponding to the 100-meV photon energy resolution.

The ion detector (microchannel plate) of our time-of-flight equipment [14] has been used to record the total ion yield spectrum. For this measurement, the exit slit width was set to 10 μm, which gave the photon energy resolution of about 45 meV.

————
*On leave from Institute of Physics, Estonian Academy of Sciences, Riia 142, EE2400 Tartu, Estonia.
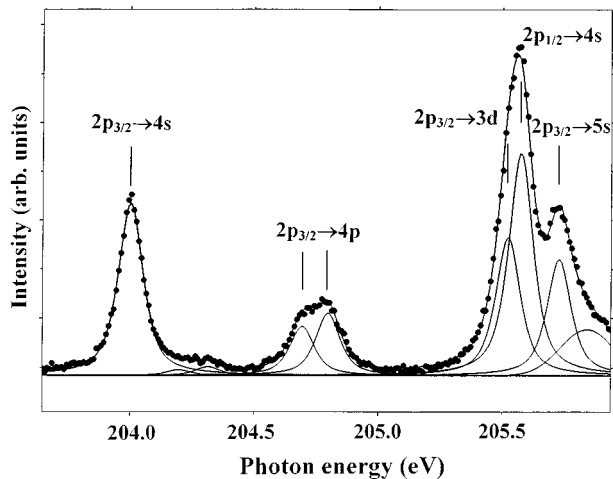
FIG. 1. Total ion yield spectrum of HCl.

III. RESULTS

A. Photoexcitation of the chlorine 2p electrons

Figure 1 presents a total ion yield spectrum of HCl, which accurately reflects the photoabsorption features. The spectrum displays the photon energy range of the Cl $2p$ excitations to the lowest Rydberg orbitals. An analogous spectrum of DCl (not presented) shows no significant differences when compared to the HCl spectrum. Photon energy has been calibrated using the energy of the $2p_{3/2} \rightarrow 4s$ excitations [204.00(3) eV] from an electron-loss spectroscopy measurement [4]. A least-squares curve fitting procedure has been applied to decompose the spectral structures and determine the energies of other peaks relative to the $2p_{3/2} \rightarrow 4s$ transitions. The assignment of peaks follows that in Ref. [4].

The decomposition results are given in Table I. The $2p_{3/2} \rightarrow 4s$ peak is described by a single Voigt profile with the full width at half maximum (FWHM) of 117(10) meV. The observed line shape is a convolution of the Lorentzian lifetime broadening with the exciting photon band. The estimated lifetime broadening is 95(10) meV, obtained by using a 45-meV Gaussian distribution for the photon band. The peak has a very weak shoulder at the high-energy side, extending more than 300 meV from the peak maximum. This is probably due to excitations to the higher vibronic levels of the $2p_{3/2}^{-1} 4s$ state.

The next $2p_{3/2} \rightarrow 4p$ structure consists of two peaks, separated by 100 meV. The $2p_{3/2} \rightarrow 3d$ and $2p_{1/2} \rightarrow 4s$ excitations contribute to the structure around 205.5 eV, which is accompanied by a high-energy peak from the $2p_{3/2} \rightarrow 5s$ excita-

TABLE I. Energies of the absorption peaks in Fig. 1.

No.	Assignment	$h\nu$ (eV)
1	$2p_{3/2} \rightarrow 4s$	204.00 [a]
2	$2p_{3/2} \rightarrow 4p$	204.695
3	$2p_{3/2} \rightarrow 4p$	204.797
4	$2p_{3/2} \rightarrow 3d$	205.526
5	$2p_{1/2} \rightarrow 4s$	205.580
6	$2p_{3/2} \rightarrow 5s$	205.731

[a]Calibrated by using Ref. [4].
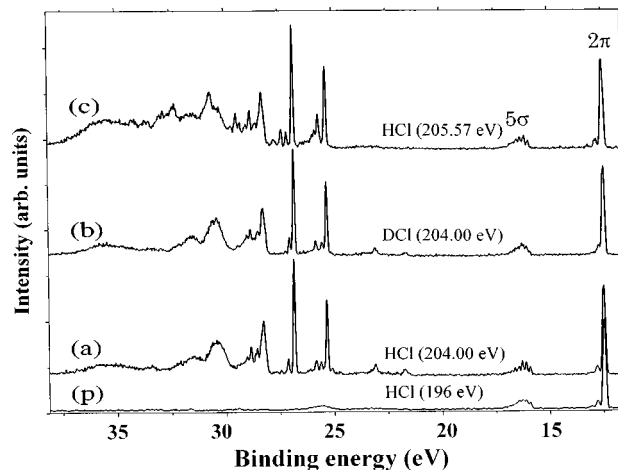
FIG. 2. Resonant Auger electron spectra of HCl, excited at 204.00- (a) and 205.57-eV (c) photon energy. The spectrum of DCl (b) is excited at 204.00 eV. The pure photoelectron spectrum of HCl (p) is excited at 196-eV photon energy.

tions. This peak has a clear asymmetry at the high-energy side and therefore requires two peaks for an acceptable fit. The line shapes for these structures (except the shoulder at 206 eV) were taken from the fit of the $2p_{3/2} \rightarrow 4s$ peak.

We will refine the assignment of the spectrum in Sec. IV C, after analyzing the resonant Auger spectra.

B. Resonant Auger spectra, general properties

Figure 2 shows the Auger electron spectra from the decay of the $2p_{3/2}^{-1} 4s$ state of HCl [curve (a)] and DCl (b), excited at 204.00-eV photon energy, and a spectrum from the decay of the overlapping $2p_{1/2}^{-1} 4s$ and $2p_{3/2}^{-1} 3d$ states in HCl, excited with 205.57-eV photons [curve (c)]. The pure photoelectron spectrum, recorded with 196-eV photons below any resonant structures, is also given as curve (p). The spectra were normalized to give equal intensities to the 2π photoelectron lines and the energy scale was calibrated using the binding energy (12.748 eV) of the 2π electrons [15].

Figure 3 presents the 25–30-eV binding energy region of the spectra in detail. This part of the spectra consists mainly of the transitions to bound molecular states housing discrete vibrational levels. Therefore the spectra display narrow well-defined line shapes, which can be analyzed by a least-squares curve fitting procedure. At first, a weak background from photoionization of the 4σ orbital and numerous correlation satellites were subtracted. Direct photoionization does not contribute remarkably to the population of the Auger final states, if compared with the resonant Auger decay. The interference between these two channels is therefore negligible and such a background subtraction is possible.

Voigt profiles with equal widths and Gaussian-to-Lorentzian ratios were used in the fit. The fitting routine produced line shapes with a 101-meV FWHM having nearly Gaussian profiles. The obtained linewidth is consistent with the Auger resonant Raman effect, [16,17] where the Auger line shape is given as a product of the photon band and Lorentzian lifetime broadening of the core-excited state, convoluted with the spectrometer broadening. Although the Voigt profile is physically incorrect in the case of pro-
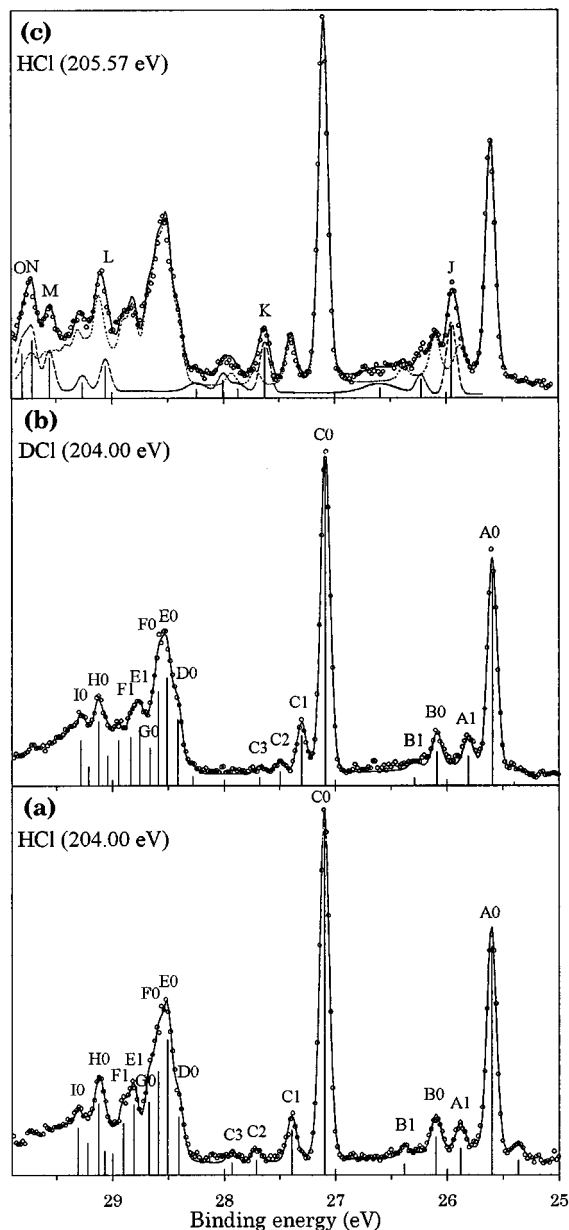
FIG. 3. The low binding energy region of spectra (a)–(c) in Fig. 2, decomposed by a least-squares curve-fitting procedure. For notations see text.

nounced Auger resonant Raman effect, it provides a sufficiently good approximation to the true line shape. The fit results are listed in Table II, with lines labeled as in Fig. 3. Line intensities are given relative to the 2π photoelectron line, which makes the line intensities in different spectra comparable, assuming that the photoelectron line is not enhanced by the participator decay channel.

C. Auger decay of the $2p_{3/2}^{-1}4s$ state

Comparison of the $2p_{3/2}^{-1}4s$ decay spectra for HCl and DCl [curves (a) and (b), respectively] shows that some of the peaks appear at nearly the same energy in both spectra, whereas the others are shifted. The former result from the transitions between the lowest vibrational levels of the initial and final electronic states of the Auger decay. The shifted

peaks in the spectra correspond to the transitions from the lowest level of the initial state to higher vibrational levels of the final state and these vibrational progressions are more closely spaced [18] in the DCl spectrum. Transitions to three different final electronic states (labeled $A-C$ in Fig. 3) are well resolved in the binding energy region up to 28 eV. These transitions populate mainly the $\nu=0$ vibrational levels of the final states, but show also some vibrational structure. In Fig. 3, the number after the label refers to the vibrational level of the final state, populated by the given transition. The vibrational progression is best resolved for electronic transition C, providing the energy spacings of 290(210), 610(400), and 830(590) meV, between the $\nu=0$ and $\nu=1-3$ levels of the final state in the HCl (DCl), respectively.

The parameters of the Voigt profiles, obtained from the fit of the transitions $A-C$, have been applied in decomposing the higher binding energy structures. The structure around 28.5 eV in Fig. 3 consists of four peaks. It is nearly identical in the spectra of HCl and DCl (see Table II), the peaks retaining their energy positions well within statistical accuracy of the fit. They have been therefore assigned as electronic transitions $D-G$. The next, weaker structure displays an apparent shift when going from the HCl to the DCl spectrum and therefore belongs to the vibrational progressions accompanying the previous structure. Based on the energy spacings and intensity ratios, the two resolved peaks of this structure come probably from the transitions E and F, involving the $\nu=1$ vibrational levels of the final states. Notably, this progression is much stronger relative to the main peaks than in the transitions $A-C$, indicating a different shape of the final-state potential energy curves. The vibrational progressions of the transitions $D-G$ are expected to continue and contribute to the spectra at the binding energies above 29 eV as enhanced background. Two more electronic transitions (H,I) seem to contribute also to the spectra above 29 eV, though their energies can be determined with rather low accuracy. Some additional (unassigned) peaks were needed to represent the enhanced background, but the uncertainty of their energies is too high to assign them either to other electronic transitions or vibrational progressions.

D. Auger decay of the $2p_{1/2}^{-1}4s$ and $2p_{3/2}^{-1}3d$ states

Both the $2p_{1/2}^{-1}4s$ and $2p_{3/2}^{-1}3d$ states were excited when recording spectrum (c) in Figs. 2 and 3, as they are separated only by 54 meV (Table I), which is smaller than our 100-meV photon bandwidth. The Auger transitions from the $2p_{1/2}^{-1}4s$ state populate the same final states as the ones from the $2p_{3/2}^{-1}4s$ state and the corresponding peaks appear at the same binding energy. On this basis, the transitions $A-I$ can be identified also in spectrum (c) of Fig. 3. The further comparison with the $2p_{3/2}^{-1}4s$ spectrum (a) shows also that the intensity distribution of at least the most intense transitions $A,C,D-F$ is very similar. On this ground, the result of the fit of the $2p_{3/2}^{-1}4s$ Auger decay spectrum has been transferred onto spectrum (c) and is shown as a dotted curve. The remaining intensity can be assigned to the decay of the $2p_{3/2}^{-1}3d$ state. The decomposition of this remaining part of the spectrum (dashed curve) is obviously much less accurate than that of the $2p_{3/2}^{-1}4s$ spectrum. Therefore only several

TABLE II. Binding and kinetic energies of the peaks in the resonant Auger electron spectra in Fig. 3. Intensities are given relative to the 2π photoelectron line. Intensity error limits are the statistical uncertainties of the fit.

No.	Peak	HCl			DCl		
		E_b (eV)	E_k (eV)	I_{rel}	E_b (eV)	E_k (eV)	I_{rel}
1	$A0$	25.60	178.40	0.79(4)	25.60	178.41	0.74(4)
2	$A1$	25.88	178.12	0.09(1)	25.81	178.19	0.10(1)
3	$B0$	26.10	177.90	0.13(1)	26.09	177.91	0.12(1)
4	$B1$	26.38	177.62	0.04(1)	26.29	177.71	0.03(1)
5	$C0$	27.10	176.90	1.22(6)	27.09	176.91	1.13(5)
6	$C1$	27.39	176.61	0.16(1)	27.31	176.70	0.17(1)
7	$C2$	27.71	176.29	0.05(1)	27.50	176.50	0.05(1)
8	$C3$	27.93	176.07	0.04(1)	27.68	176.32	0.03(1)
9	$D0$	28.41	175.59	0.20(3)	28.42	175.58	0.23(4)
10	$E0$	28.51	175.49	0.47(8)	28.51	175.49	0.38(6)
11	$F0$	28.59	175.41	0.36(5)	28.59	175.41	0.33(5)
12	$G0?$	28.68	175.32	0.25(7)	28.67	175.34	0.13(4)
13	$E1$	28.81	175.19	0.24(2)	28.76	175.24	0.20(3)
14	$F1$	28.91	175.09	0.18(3)	28.84	175.16	0.17(4)
15	$H0$	29.13	174.87	0.25(5)	29.13	174.87	0.22(5)
16	$I0?$	29.31	174.69	0.16(5)	29.29	174.71	0.16(5)
17	J	25.95	179.616	0.26			
18	K	27.63	177.942	0.18			
19	L	29.06	176.512	0.12			
20	M	29.56	176.010	0.15			
21	N	29.71	175.857	0.21			
22	O	29.80	175.766	0.16			

most intense lines have been labeled (J–O) and are listed in Table II, but no attempt has been made to identify the vibrational structures.

The contribution to the resonant Auger spectrum from the decay of the $2p_{3/2}^{-1}3d$ state is rather small in the binding energy region of Fig. 3, but Fig. 2 shows a strong intensity enhancement above 30 eV. Using the 2π photoelectron line for the intensity normalization, we found that the Auger structures in spectrum (c) have nearly twice the intensity of the $2p_{3/2}^{-1}4s$ spectrum (a).

IV. DISCUSSION

A. Auger decay of the $2p_{3/2}^{-1}4s$ state

The strict spectator model can be applied as the first approximation in the analysis of the resonant Auger spectra. The coupling of the excited electron in a Rydberg orbital to the open shell structure, created by the Auger decay in the molecule, is neglected in this model. This electron in the Rydberg orbital just acts as a shield, which lowers the total energy of the electron configuration. The resonant Auger spectrum should thus have a structure, identical to the normal Auger (parent) spectrum from the decay of the $2p^{-1}$ core-ionized state, the peaks being shifted to higher kinetic energies from the parent peaks.

A comparison with the normal Auger spectrum [9,19] helps to clarify the overall structure of the spectra [(a),(b)] in Fig. 2. The broad features around 36, 31.5, and 30.5 eV arise from the transitions to the states that are related to the

$5\sigma^{-2}(^1\Sigma^+)$, $5\sigma^{-1}2\pi^{-1}(^1\Pi)$, and $5\sigma^{-1}2\pi^{-1}(^3\Pi)$ parent states, respectively. These states are of dissociative nature, giving broad Auger line shapes with no vibrational structure. The lines are shifted by 5–6 eV to higher kinetic energies, as compared with the parent structures in the normal Auger spectrum.

The sharp peaks at lower binding energies (Fig. 3) are related to the transitions to bound states having $2\pi^{-2}$ parent configuration. Peaks A and C correspond nicely to the $2p_{3/2}^{-1}\rightarrow2\pi^{-2}(^3\Sigma^-)$ and $2p_{3/2}^{-1}\rightarrow2\pi^{-2}(^1\Delta)$ parent transitions in the normal Auger spectra, having nearly the same energy splitting (1.50 eV) and similar intensity ratio. Representation of the third term ($^1\Sigma^+$) of the parent $2\pi^{-2}$ configuration is not obvious. Following the spectator model and single configuration picture, the resonant Auger final state should be $2\pi^{-2}(^1\Sigma^+)4s(^2\Sigma^+)$. However, the existence of only one state with the $2\pi^{-2}(^1\Sigma^+)4s$ character is hampered because of the pronounced many-electron nature of this state, as seen also in photoelectron spectroscopy. Namely, the inner valence photoelectron spectra [20,21] show a rich structure in the binding energy region above 20 eV, which borrows intensity from the transitions to the $4\sigma^{-1}(^2\Sigma^+)$ state due to strong configuration interaction. Calculations [20,22] have shown that the three HCl$^+$ states of $^2\Sigma^+$ symmetry with the lowest energy have repulsive potential energy curves, but the fourth $^2\Sigma^+$ state is bonding and can be assigned to the structure at 28.5-eV binding energy in the photoelectron spectrum. In our resonant Auger spectra, the intense structure around 28.5 eV incorporates four electronic

transitions $D-G$. One of them, most probably E, can be assigned to the transitions to the fourth $^2\Sigma^+$ HCl$^+$ final state, which can be tentatively labeled as $2\pi^{-2}(^1\Sigma^+)4s(^2\Sigma^+)$, if one wishes to retain the strict spectator model.

The assignment of the remaining transitions B, D, and $F-I$ cannot be derived directly from the normal Auger spectrum. Especially the complex structure $(D-I)$ in the high binding energy side of Fig. 3 indicates that there is a strong redistribution of the Auger line intensities in this energy region. Strong mixing of the $^2\Sigma^+$ final states is most probably responsible for this effect. The fourth $^2\Sigma^+$ state has been already seen to mix with the $4\sigma^{-1}(^2\Sigma^+)$ state. We would also like to cite Ref. [22], where the fourth $^2\Sigma^+$ state was expected to ''exhibit a high degree of Rydberg character and considerable configuration mixing with the many states that lie in close proximity.'' Calculations with an extended basis set including not only the $4\sigma^{-1}$ and $2\pi^{-2}4s$ configurations, but also the higher members as the $2\pi^{-2}ns, n=5,6, \ldots$ and $2\pi^{-2}nd, n=3,4, \ldots$ configurations would be needed to treat the effect in detail. It is possible that peak B appears also because of the final-state configuration interaction.

A rather similar effect has been observed also in the $2p^{-1}4s \rightarrow 3p^{-2}4s$ resonant Auger spectrum of argon [6]. MCDF calculations [7] have shown that there is a strong mixing between energetically overlapping $3p^{-2}4s$ and $3p^{-2}3d$ final-state configurations, which is responsible for the appearance of a large number of lines in the Auger electron spectra.

The total intensity of the structure $(D-I)$ is notably higher than could be expected on the basis that only the intensity from the Auger transitions to the $2\pi^{-2}(^1\Sigma^+)4s(^2\Sigma^+)$ state is redistributed. The transitions to the $2\pi^{-2}(^1\Sigma^+)$ parent state have the intensity of about 50% relative to the transitions to the $2\pi^{-2}(^1\Delta)$ state in the normal Auger spectrum [9], whereas the total intensity of transitions $D-I$ realtive to transition C is clearly higher in the present spectra. If configurations such as $5\sigma^{-2}nl$ and $5\sigma^{-1}2\pi^{-1}nl$ are also involved in the mixing, then the intensity enhancement could be understood, as the transitions to some of these states are expected to be quite intense.

In argon, the $2p^{-1}4s \rightarrow 3p^{-2}5s$ shakeup processes have been found to be important, having as much as about 10% of the total transition probability [7]. These processes yield peaks at higher binding energies than the spectator Auger transitions in the Auger electron spectrum. The shakeup mechanism can play some role also in the spectra of HCl(DCl), where the estimated shift of the shakeup peaks from the spectator peaks is about 3.8 eV [5]. The shake processes were assigned an important role in the previous study, [5] but the present high-resolution results suggest that the final-state configuration interaction is the dominating effect, redistributing line intensity in the spectra.

B. Auger decay of the $2p_{3/2}^{-1}3d$ state

Most of the intensity of spectrum (c) in Fig. 3 originates from the decay of the $2p_{1/2}^{-1}4s$ state. Only the transitions $J-O$ together with increased background appear as new. The $2p^{-1}3d \rightarrow 3p^{-2}3d$ resonant Auger spectra of argon show a very strong coupling between the $3d$ electron and the re-

maining part of the final-state electronic configuration, due to the collapsed nature of the $3d$ orbital. This leads to the complete breakdown of the strict spectator model, so that a large number of peaks appears in the spectrum, spread over a wide energy range, much exceeding the range of the $3p^{-2}4s$ configuration. This seems to be the situation also in the case of HCl, where the assigment of such peaks needs accurate calculations to be performed. Naturally, the configuration interaction effects should be reflected in the $2p_{3/2}^{-1}3d$ decay spectrum too.

The enhanced intensity of the spectrum at higher binding energy suggests that most of the intensity from the decay of the $2p_{3/2}^{-1}3d$ state is distributed in this region, where the bound states related to the $2\pi^{-2}3d$ configuration overlap with the states from the $5\sigma^{-1}2\pi^{-1}3d$ and $5\sigma^{-2}3d$ configurations. The $3d \rightarrow 4d$ shakeup transitions have been found to be exceptionally strong (about 50% from the total intensity) in argon due to the collapse of the $3d$ orbital [7]. Such shakeup processes would redistribute the intensity in the resonant Auger spectra towards higher binding energies.

C. Properties of the core-excited states

So far we have used the atomic relativistic $2p_{1/2}$ and $2p_{3/2}$ notations for the Cl $2p$ core orbital, as it has a pronounced atomic character and is split by strong spin-orbit interaction. In the molecule, the molecular field causes an additional splitting of the $2p_{3/2}$ component, so that three core-ionized states were observed in the $2p$ photoelectron spectrum of HCl and DCl [9]. Using the usual molecular orbital notation, the three orbitals involved are $1\pi_{1/2}$ (from $2p_{1/2}$), and $3\sigma_{1/2}$ and $1\pi_{3/2}$ (from $2p_{3/2}$). The spin-orbit splitting of the π-orbital was found to be 1.665 eV and the molecular field splitting between the $3\sigma_{1/2}$ and $1\pi_{3/2}$ orbitals 80 meV. The orbital with the lowest energy is $1\pi_{1/2}$, followed by $3\sigma_{1/2}$ and $1\pi_{3/2}$. Although the λ notation is not good for the core orbitals with strong spin-orbit and weak molecular field splitting, it represents qualitatively the observed tendency of the orbitals towards the σ- and π-like characters.

The $2p_{3/2}^{-1}4s$ core-excited state is also split into the $1\pi_{3/2}^{-1}4s$ and $3\sigma_{1/2}^{-1}4s$ states by the molecular field, as well as the other $2p_{3/2}$ core-excited states. The $2p_{3/2} \rightarrow 4p$ excitation shows indeed two components in the absorption spectrum (Fig. 1), which can be assigned to the molecular field splitting. Here, the $4p$ orbital also has the σ and π components, which complicates the assignment. The $2p_{3/2} \rightarrow 4s$ excitation is, on the contrary, represented by only one component in the absorption spectrum. The decomposition using only one component also for the $2p_{3/2} \rightarrow 3d$ transitions gave a splitting of 1.58 eV between the $2p_{3/2} \rightarrow 4s$ and $2p_{1/2} \rightarrow 4s$ transition energies. This is exactly the splitting between the $3\sigma_{1/2}^{-1}$ and $1\pi_{1/2}^{-1}$ core-ionized states. An attempt to decompose the spectrum in Fig. 1 using a splitting of 1.665 eV (the splitting between the $1\pi_{3/2}^{-1}$ and $1\pi_{1/2}^{-1}$ states) requires two components for the $2p_{3/2} \rightarrow 3d$ transitions and gives a strongly suppressed intensity for the $2p_{1/2} \rightarrow 4s$ excitation. This contradicts the results from the resonant Auger spectum (c) in Figs. 2 and 3, where the $2p_{1/2}^{-1}4s$ decay gives a large contribution. Therefore, the observed peaks can be most probably assigned

as the excitations $2p_{3/2}(3\sigma_{1/2})\rightarrow 4s$ at 204.00 eV and $2p_{1/2}(1\pi_{1/2})\rightarrow 4s$ at 205.58 eV, whereas the $2p_{3/2}(1\pi_{3/2})\rightarrow 4s$ excitation is missing. (The weak high-energy shoulder in the spectrum extends too far to be ascribed to the second molecular field-split component.) The $2p$ holes of the core-excited states do not necessarily inherit the spatial orientation of the core-ionized states, as the Rydberg electron makes different mixing of states possible. Forthcoming angle-resolved measurements might help to clarify these matters.

The photoionization cross sections for the three $2p$ molecular field-split components are equal [9]. The lack of one $2p_{3/2}$ component thus explains the nearly equal intensities of the $2p_{3/2}\rightarrow 4s$ and $2p_{1/2}\rightarrow 4s$ excitations in the absorption spectrum, instead of having the 2:1 statistical ratio as, e.g., in the case of argon.

A similar refinement for the $2p\rightarrow 3d$ transitions must take into account also the three components (σ, π, and δ) of the $3d$ Rydberg orbital. It looks like in this case one excitation dominates as well, but calculations that take fully into account the molecular field effects and the spin-orbit interaction are required to proceed further.

V. CONCLUSIONS

A number of electronic transitions to the $2\pi^{-2}nl$ final states have been found in the $2p_{3/2}^{-1}4s$ resonant Auger spectra of the HCl and DCl molecules. The transitions are accompanied by vibrational progressions, showing clearly different characteristics in the spectra of HCl and DCl due to isotopic effects. The most intense electronic transitions follow the strict spectator model quite well, whereas the rest can be assigned to the transitions that have become available via the final-state configuration interaction. The shakeup processes have been found to play a minor role in this resonance.

The strict spectator model breaks down in the decay of the $2p_{3/2}^{-1}3d$ state. The Auger electron spectrum shows, after removing the contribution from the $2p_{1/2}^{-1}4s$ decay, that most of the intensity is distributed in the binding energy region above 30 eV. The intensity transfer to this region can be provided by an exceptionally strong shakeup mechanism. The resonance Auger spectra indicate also that both the energetically overlapping $2p_{3/2}^{-1}3d$ and $2p_{1/2}^{-1}4s$ initial states have considerable photoabsorption cross sections.

The molecular field splits the excitations from the $2p_{3/2}$ core to the $4s$ Rydberg orbital into two components. Only one component has been found in the photoabsorption and has been assigned as the $2p_{3/2}(3\sigma_{1/2})\rightarrow 4s$ excitation. The transitions from the other component, $2p_{3/2}(1\pi_{3/2})\rightarrow 4s$, have not been observed.

[1] W. H. E. Schwarz, Chem. Phys. **11**, 217 (1975).

[2] K. Ninomiya, E. Ishiguro, S. Iwata, A. Mikuni, and T. Sasaki, J. Phys. B **14**, 1777 (1981).

[3] H. Aksela, S. Aksela, M. Hotokka, A. Yagishita, and E. Shigemasa, J. Phys. B **25**, 3357 (1992).

[4] D. A. Shaw, D. Cvejanović, G. C. King, and F. H. Read, J. Phys. B **17**, 1173 (1984).

[5] A. Kivimäki, H. Aksela, S. Aksela, A. Yagishita, and E. Shigemasa, J. Phys. B **26**, 1 (1993).

[6] J. Mursu *et al.* (unpublished).

[7] H. Aksela and J. Mursu, Phys. Rev. A **54** (to be published).

[8] Z. F. Liu, G. M. Bancroft, K. H. Tan, and M Schachter, J. Electron Spectrosc. Relat. Phenom. **67**, 299 (1994).

[9] H. Aksela, E. Kukk, S. Aksela, O.-P. Sairanen, A. Kivimäki, E. Nõmmiste, A. Ausmees, S. J. Osborne, and S. Svensson, J. Phys. B **28**, 4259 (1995).

[10] S. Aksela, A. Kivimäki, A. Naves de Brito, O.-P. Sairanen, S. Svensson, and J. Väyrynen, Rev. Sci. Instrum. **65**, 831 (1994).

[11] S. Aksela, A. Kivimäki, O.-P. Sairanen, A. Naves de Brito, E. Nõmmiste, and S. Svensson, Rev. Sci. Instrum. **66**, 1621 (1995).

[12] S. Aksela, A. Kivimäki, R. Nyholm, and S. Svensson, Rev. Sci. Instrum. **63**, 1252 (1992).

[13] S. J. Osborne, A. Ausmees, J. O. Forsell, B. Wannberg, G. Bray, L. B. Dantas, S. Svensson, A. Naves de Brito, A. Kivimäki, and S. Aksela, Synchrotron Radiat. News **7**, 25 (1994).

[14] J. Jauhiainen, S. Aksela, and E. Nõmmiste, Phys. Scr. **51**, 549 (1995).

[15] K. P. Huber and G. Herzberg, *Constants of Diatomic Molecules* (Van Nostrand, New York, 1979).

[16] S. Aksela, E. Kukk, H. Aksela, and S. Svensson, Phys. Rev. Lett. **74**, 2917 (1995).

[17] E. Kukk, S. Aksela, and H. Aksela, Phys. Rev. A **53**, 3271 (1996).

[18] L. Karlsson, P. Baltzer, S. Svensson, and B. Wannberg, Phys. Rev. Lett. **60**, 2473 (1988).

[19] S. Svensson, L. Karlsson, P. Baltzer, M. P. Keane, and B. Wannberg, Phys. Rev. A **40**, 4369 (1989).

[20] M Hiyama and S. Iwata, Chem. Phys. Lett. **210**, 187 (1993).

[21] S. Svensson, L. Karlsson, P. Baltzer, B. Wannberg, U. Gelius, and M. Y. Adam, J. Chem. Phys. **89**, 7193 (1988).

[22] A. D. Pradhan, K. P. Kirby, and A. Dalgrano, J. Chem. Phys. **95**, 9009 (1991).